E-Textile Origami Dipole Antennas with Graded Embroidery for Adaptive RF Performance

Saad Alharbi, Shreyas Chaudhari, Abdullahi Inshaar, Hamil Shah, Chengzhe Zou,
Ryan L. Harne and Asimina Kiourti

Abstract— **We present a new class of reconfigurable origami-based antennas formed by embroidered conductive E-threads. State-of-the-art techniques used to realize origami antennas employ fragile conductive inks and/or copper tape. By contrast, the proposed approach brings forward enhanced robustness and durability as attributed to the inherent strength of the E-threads. To facilitate folding along the creases while also providing Radio-Frequency (RF) performance close to that of copper, a graded embroidery process is proposed. The grading scheme uses a density of 7 E-threads/mm on the antenna and a reduced density around the creases (as few as 1 E-thread/mm in this study). Proof-of-concept results for an accordion-based dipole antenna tunable from 760 to 1015 MHz show excellent agreement between simulations and measurements for all E-textile prototypes and the copper equivalent. Notably, embroidery density at the creases can be reduced to as low as 1 E-thread/mm without apparent degradation in the RF performance. Overall, the E-textile origami antennas may transform opportunities for reconfigurable antennas to be leveraged in wearable and structural applications.**

Index Terms— **E-textiles, embroidered antennas, flexible antennas, origami structures, reconfigurable antennas.**

I. INTRODUCTION

RECONFIGURABLE antennas have been extensively explored in recent years for a wide range of applications that include satellite communications, radars, and wearable wireless systems, among others [1]-[7] As an example, the ever-increasing requirement for a single device to accommodate a multitude of services/applications at different frequencies (e.g., WiFi, Bluetooth, GSM, LTE, GPS) implies the need for antennas that can reconfigure their operating frequency and, hence, their Radio-Frequency (RF) performance [1]. Accordingly, diverse techniques have been reported to enable antenna reconfiguration, including both electrical and mechanical approaches [3].

TABLE I
SUMMARY OF ORIGAMI ANTENNAS REPORTED IN THE LITERATURE VS. THE PROPOSED APPROACH

Ref.	Antenna type	Frequency range (GHz)	Substrate material	Conductive material
[12]	Helical	0.86 – 2.14	Paper	Copper foil
[13]	Helical	4 – 4.5	Plastic	Copper wire
[14]	Monopole array	2 – 4	Paper	Copper tape
[15]	Helical	2.07 – 4.45	Paper	Copper tape
[16]	Microstrip patch	2 – 2.3	SMPs	Copper foil
[17]	Yagi-Uda loop array	1.31	Paper	Copper tape
[18]	Patch array	2.3	SMPs	Conductive ink
Proposed	Dipole	0.76 – 1.015	Fabric	E-threads

In particular, origami-based antenna structures [8], [9] that fold and unfold are shown to manipulate RF performance by way of the shape reconfiguration [10]-[12]. Yet, origami-based antennas reported to date exhibit limited durability as attributed to the fragility of their constituent materials, Table I [12]-[18]. Specifically, copper tape and conductive inks are conventionally used to realize the conductive portions of state-of-the-art origami antennas. Following extensive mechanical stress that is typically associated with origami folding [12], the former material is prone to delamination while the latter is prone to cracking and deterioration in conductivity [19]. Regarding the antenna substrate, paper and shape memory polymers (SMPs) have been employed. Though low-cost, recyclable, and readily available, paper is not robust to extensive folding. In addition, paper is influenced by environmental factors (humidity, etc.), which in turn alter its dielectric properties (permittivity, loss tangent) and life expectancy. SMPs, i.e., polymers that convert into pre-programmed structures under certain stimuli [16], are more robust than paper, but have limited means to adhere to conductors.

To address these shortcomings, here we introduce a framework for a novel class of reconfigurable origami-based antennas that are durable and robust. Our approach relies on automated embroidery of conductive E-threads upon fabric substrates. Our previous work has demonstrated the mechanical robustness and thermal tolerance associated with embroidered E-textiles [20]. Here, E-thread embroidery is leveraged to realize origami antennas that fold/unfold to adapt

RF performance. To facilitate folding across the creases while also providing surface conductivity close to that of copper, a graded embroidery process is proposed. The process employs graded densities of embroidery to ease folding at crease lines and boost conductivity on the extended antenna surface. As a proof-of-concept, an accordion-based dipole origami antenna is explored, tunable across the 760 to 1015 MHz frequency range. Measurements are presented to establish the effectiveness of the embroidery process. To exemplify the adaptive antennas, simulations and measurements are contrasted for the accordion dipoles, while contrasts to a solid copper-based antenna illustrate the efficacy of the concept in comparison to conventional antenna material selection. Excellent agreement exists for all aforementioned prototypes, highlighting the feasibility and potential of our approach.

II. GRADED EMBROIDERY PROCESS

The block diagram of the proposed graded embroidery process used to realize E-textile origami antennas is shown in Fig. 1. The block diagram is presented within the framework of realizing an accordion-based dipole antenna. The framework can be generalized to embroider diverse origami structures. As a first step, the origami antenna is designed by computer modeling to understand ideal performance characteristics (e.g., Ansys HFSS [21] or COMSOL Multiphysics® [22]). The unfolded antenna geometry is subsequently considered. The locations of creases are identified and marked with a ~1cm-wide area across crease centers. The aforementioned width is selected so as to clearly differentiate the creased areas following antenna embroidery, and is related to the particular E-threads and tension used in the embroidery process. In our case, 7-filament Elektrisola E-threads [23] were employed at a tension of 4.5 (unit-less quantity used to quantify pulling stress on a Brother 4500D embroidery machine with a 1 to 6 tension scale). The selected E-threads exhibit a low DC resistance of 1.9 Ω/m, and a diameter of only 0.12 mm that enables embroidery precision as high as ~0.1 mm [24]. Next, a Windows Metafile (WMF) of the aforementioned design is created, and further imported into Brother's Personal Embroidery Design Software System (PE-DESIGN) for digitization [25]. Digitization implies identification of the path that the needle will follow during embroidery, stitch by stitch. That is, at this point, the embroidery density can be manually adjusted. For high surface conductivity, comparable to that of copper, we propose a density of 7 E-threads/mm upon the antenna except for the creases. The aforementioned density is the maximum supported by the embroidery machine. Concurrently, and in order to facilitate folding, a reduced density is selected for the 1-cm-wide areas that immediately surround the creases. This density is subject to optimization in this study.

It is expected that lower densities will be more favorable to folding, yet will be associated with lower surface conductivity values. To verify the latter, four 50 Ω transmission lines (TLs) were fabricated and tested, as shown in Fig. 2. All TLs were 5 cm long and employed a copper ground plane and a felt substrate, yet differed by the material used to realize the TL. The latter was, respectively, selected as: (a) copper, (b) E-threads embroidered at a density of 7 E-threads/mm, (c) E-
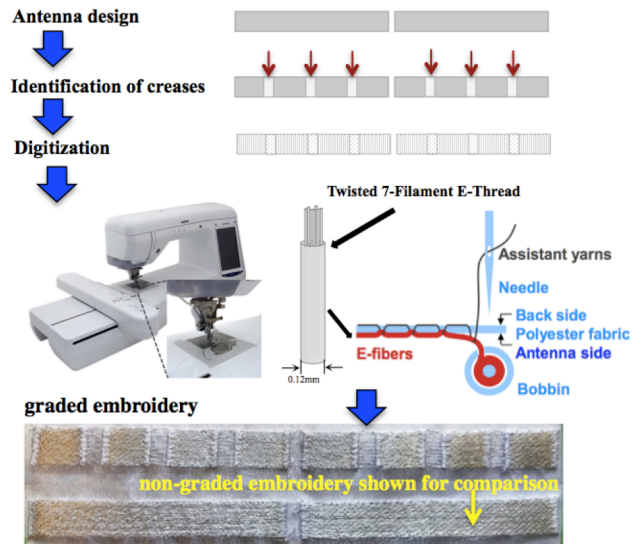

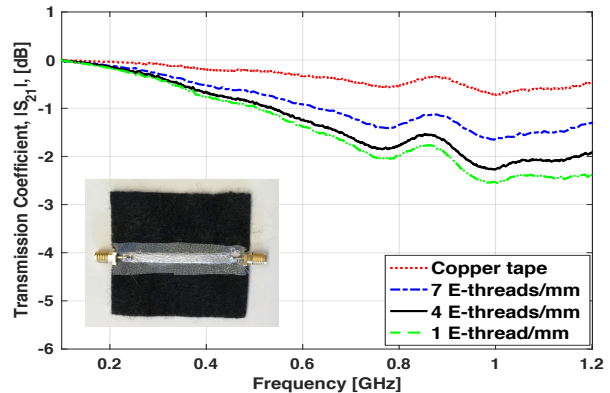Fig. 1. Proposed graded embroidery process.

Fig. 2. Transmission coefficient, |S$_{21}$|, performance for 50 Ω TL prototypes with TLs made of copper and E-threads embroidered at a density of 7, 4, and 1 E-threads/mm.

threads embroidered at 4 E-threads/mm, and (d) E-threads embroidered at 1 E-thread/mm. The transmission coefficient performance of all TLs is plotted in Fig. 2 as a function of frequency. E-textiles exhibit slightly higher losses than copper, with reduced E-thread density leading to greater loss. Though Fig. 2 plots the 0.1 to 1.2 GHz frequency range that is of most relevance to this particular study, similar results can be obtained for up to 4 GHz. Beyond 4 GHz, surface roughness associated with E-textiles further increases the loss in comparison to copper [24], [26]. It is thus concluded that reduced E-thread density should be employed sparsely only across the creases to ease folding of origami antennas.

III. VALIDATION FOR A PROOF-OF-CONCEPT ACCORDION-BASED ORIGAMI DIPOLE

A. Antenna Prototypes and Measurement Set-Up

To validate the adaptive embroidery process of Fig. 1, a proof-of-concept accordion-based origami dipole is explored. As shown in Fig. 1 and Fig. 3, a half-wavelength dipole is employed which exhibits an overall length of ~165 mm, a width of ~10 mm, and three creases upon each arm. Though a single fold across each arm will be explored in this
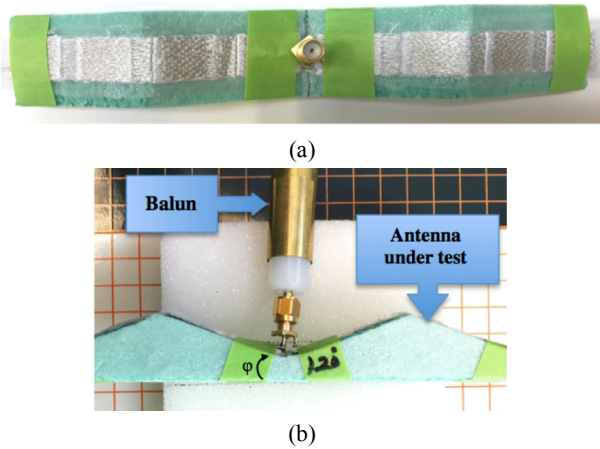
Fig. 3. E-textile accordion- dipole placed on a Styrofoam fixture: (a) top view, and (b) measurement set-up on the RFxpert.

study, this prototype may eventually be folded across each of the realized creases. For comparison purposes, four dipole prototypes are fabricated and tested. The first prototype is a prototype made of copper tape. The second prototype employs a conventional non-graded embroidery process at a uniform density of 7 E-threads/mm (shown at the bottom of Fig. 1). The third and fourth prototypes employ a density of 7 E-threads/mm upon the antenna surface and a reduced density of 4 and 1 E-threads/mm at the creases, respectively (see Fig. 1 and Fig. 3(a)). The prototypes are embroidered upon organza that has dielectric properties (permittivity, loss tangent) similar to air. The copper is adhered to the organza by means of an adhesive-backed copper tape. However, other fabrics may alternatively be used as a substrate (e.g., Kevlar, cotton, or felt). Accordingly, other conductive threads, besides Elektrisola, may be employed [27], [28].

Measurements are conducted with antennas placed on styrofoam fixtures with fold angles $\varphi = 0$ (unfolded), 20°, 40°, and 60°, Fig. 3. A laser cutter is used to form the styrofoam fixtures to ensure dimensional precision. The antennas are securely taped upon the fixtures using a lossless tape with permittivity close to air. Reflection coefficient and realized gain measurements are taken via a network analyzer and EMScan's RFxpert [29], respectively. To connect the balanced dipole to the unbalanced coaxial cable, bazooka baluns tuned at the antennas' resonance frequencies are used. For validation, measurement results are compared with Finite Element (FE) simulations for an equivalently shaped copper dipole antenna in ANSYS HFSS [21].

B. Simulation and Measurement Results

Reflection coefficient results (measured and simulated) for different folding angles φ are shown in Fig. 4 as a function of frequency. As the antenna folds, the projected length reduces, and the resonance frequency increases. This is highlighted in Fig. 5 that plots the surface currents upon the copper-based simulated dipole for different folding angles. Specifically, the antenna resonance frequency changes as ~760, ~790, ~860, and ~1015 MHz for $\varphi = 0^o$ (flat), 20°, 40°, and 60°, respectively. Good agreement is achieved between the data and simulations, with a discrepancy of <0.6% in the achieved resonance frequencies. The 10-dB bandwidth is measured as
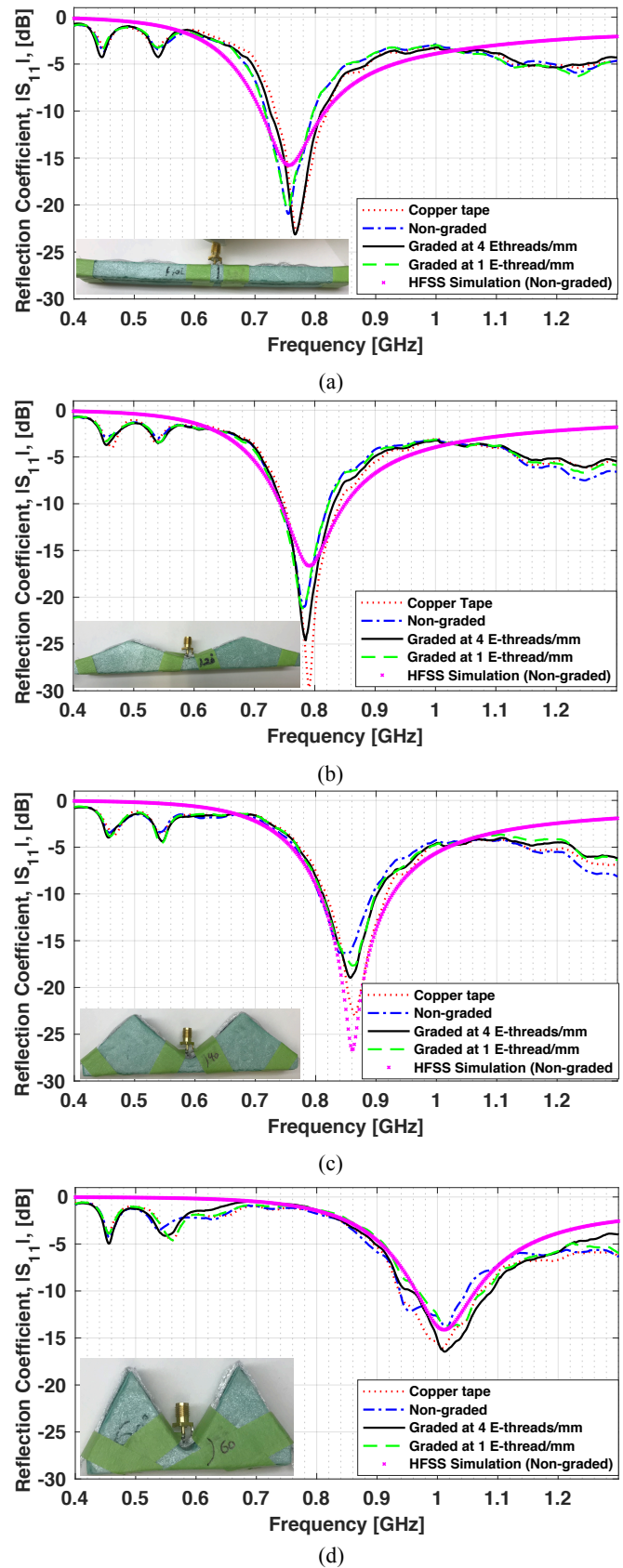

Fig. 4. Measured and simulated reflection coefficient, $|S_{11}|$, of the accordion-based dipole prototypes when: (a) $\varphi = 0^o$ (flat), (b) $\varphi = 20^o$, (c) $\varphi = 40^o$, and (d) $\varphi = 60^o$.
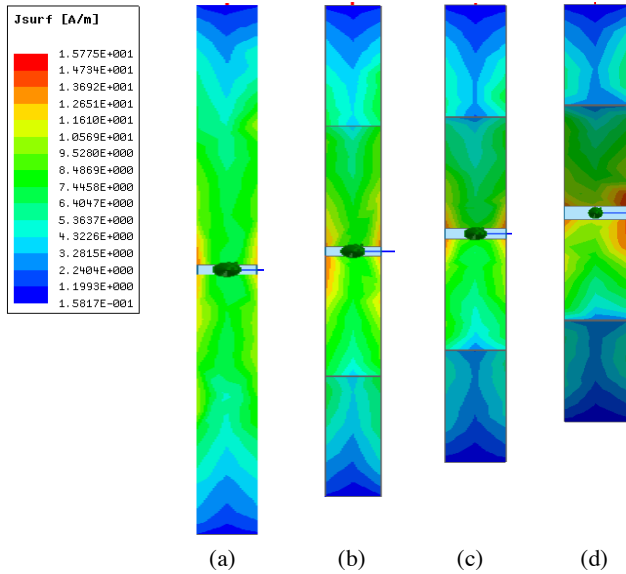
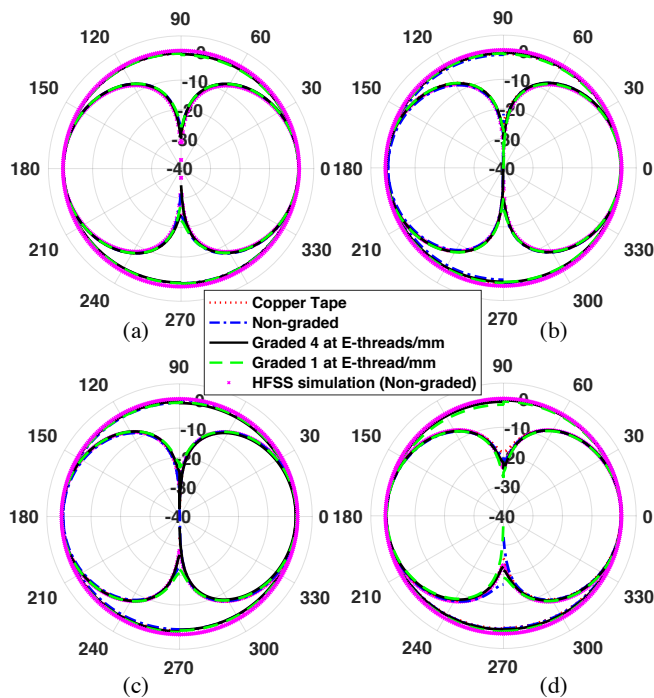Fig. 5. Simulated surface current upon the accordion-based dipole when: (a) φ = 0° (flat), (b) φ = 20°, (c) φ = 40°, and (d) φ = 60°.

Fig. 6. E- and H-plane radiation patterns of the accordion-based dipole when: (a) φ = 0° (flat), (b) φ = 20°, (c) φ = 40°, and (d) φ = 60°.

~118, ~108, ~103, and ~100 MHz for φ = 0° (flat), 20°, 40°, and 60°, respectively, with a variation of <10% among all four prototypes and simulations. These results demonstrate that reconfiguration of the E-textile origami dipoles enables a wide range of change in resonance frequency while maintaining around 84% of the initial 10-dB bandwidth.

The E- and H-plane radiation patterns for all antenna prototypes are shown in Fig. 6 and further compared vs. the corresponding simulation results. Again, excellent agreement is observed between the simulations and measurements.
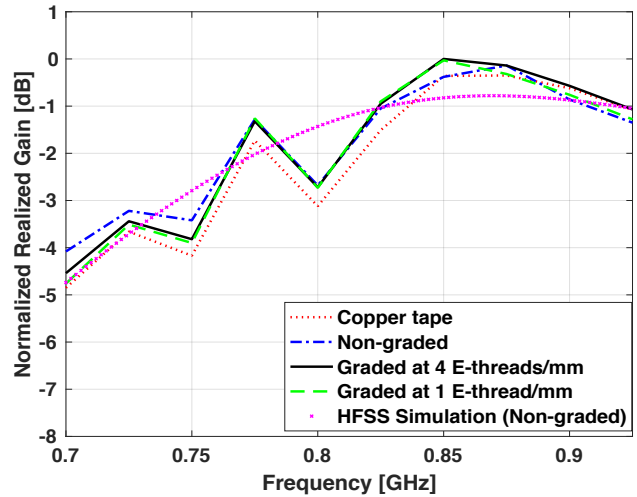

Fig. 7. The normalized realized gain for the accordion-based dipole on the 40° bend.

Discrepancies are smaller than 0.2, 0.4, 0.5, and 0.7 dB for φ = 0°, 20°, 40°, and 60°, respectively. Increasing measurement errors with folding angles are associated with difficulties in feeding the antenna since the feed point coincides with a valley in the styrofoam fixture, Fig. 3(b). The normalized maximum realized gain as a function of frequency for the example case of φ = 40° is shown in Fig. 7. Here, the difference   between all measured prototypes is within ~0.35 dB error, while the difference between measurements and simulations is within ~1 dB error, both of which lie within the measurement error range of the RFxpert. Combined with the experimental results of Fig. 4, 6, and 7, it is evident that embroidery densities of 7 E-threads/mm and 1 E-thread/mm at the antenna and creases, respectively, provide easy folding without apparent influence on performance.

IV. CONCLUSION

A novel class of origami antennas fabricated via adaptive embroidery of conductive E-threads was introduced and validated. To facilitate folding while retaining the RF performance, the embroidery density was reduced at the fold creases. Feasibility of the proposed approach was demonstrated using an accordion-based dipole antenna geometry. By folding the dipole, the resonant frequency was shifted from 760 to 1015 MHz while retaining 84% of the original 10-dB bandwidth. Measurements for different E-thread densities along the creases showed excellent agreement, as also compared vs. copper equivalents. Embroidery densities of 7 and 1 E-threads/mm at the antenna and creases, respectively, were identified as optimal.

Overall, the proposed E-textile origami antennas introduce opportunities to quantify deformation in many applications by way of reversible change in RF properties. The presented fabrication method is applicable to several types of origami antennas. Future work will focus on deploying techniques to fold/unfold the antenna as an alternative to Styrofoam fixtures employed in this work, as well as sophisticated origami antenna designs.

REFERENCES

[1] N. Haider, D. Caratelli, A. G. Yarovoy, "Recent developments in reconfigurable and multiband antenna technology," Int. J. Antennas Propag., 2013.

[2] R. L. Haupt, M. Lanagan, "Reconfigurable antennas," IEEE Antennas Propag. Mag., vol. 55, no. 1, pp. 49-61, Feb. 2013.

[3] J. Costantine, Y. Tawk, S. E. Barbin, C. G. Christodoulou, "Reconfigurable antennas: Design and applications," Proc. IEEE, vol. 103, no. 3, pp. 424-437, Mar. 2015.

[4] S.M. Saeed, C.A. Balanis, C.R. Birtcher, A.C. Durgun, and H.N. Shaman, "Wearable flexible reconfigurable antenna integrated with artificial magnetic conductor," IEEE Antennas Wireless Propag. Lett., vol. 16, pp. 2396-2399, Jun. 2017.

[5] S. Yan and G.A.E. Vandenbosch, "Radiation pattern-reconfigurable wearable antenna based on metamaterial structure," IEEE Antennas Wireless Propag. Lett., vol. 16, pp. 1715-1718, Feb. 2016.

[6] H. Giddens, L. Yang, J. Tian, and Y. Hao, "Mid-infrared reflect-array antenna with beam switching enabled by continuous graphene layer," IEEE Photon. Technol. Lett., vol. 30, no. 8, pp. 748-751, Apr. 2018.

[7] H. Wang, Y. Wang, et al., "Small-size reconfigurable loop antenna for mobile phone applications," IEEE Access, vol. 4, pp. 5179-5186, Jul. 2016.

[8] R.L. Harne and D.T. Lynd, "origami acoustics: using principles of folding structural acoustics for simple and large focusing of sound energy," Smart Mat. Structur, vol. 25, p. 085031, 2016.

[9] D.T. Lynd and R.L. Harne, "Strategies to predict radiated sound fields from foldable, Miura-ori-based transducers for acoustic beamfolding," J. Acoust. Soc. Amer., vol. 141, pp. 480-489, 2017.

[10] M. Nogi, N. Komoda, K. Otsuka and K. Suganuma, "Foldable Nanopaper Antennas for origami Electronics," Nanoscale, vol. 5, pp. 4395–4399, 2013.

[11] C. Zou, S. Chaudhari, S. Alharbi, H. Shah, A. Kiourti, and R.L. Harne, "Investigation of Reconfigurable Antennas by Foldable, E-Textile Tessellations: Modeling and Experimentation," in Proc. 175th Meet. Acoust. Soc. Amer., Minneapolis, MN, May 7–11, 2018.

[12] X. Liu, S. Yao, B. S. Cook, M. M. Tentzeris and S. V. Georgakopoulos, "An origami Reconfigurable Axial-Mode Bifilar Helical Antenna," IEEE Tran. Antennas Propag., vol. 63, no. 12, pp. 5897-5903, Dec. 2015.

[13] S. J. Mazlouman, A. Mahanfar, C. Menon, and R. G. Vaughan, "Reconfigurable axial-mode helix antennas using shape memory alloys," IEEE Trans. Antennas Propag., vol. 59, no. 4, pp. 1070–1077, Apr. 2011.

[14] S.I.H Shah, D. Lee, M. Tentzeris, and S. Lim, "A Novel High-Gain Tetrahedron origami," IEEE Antennas Wireless Propag. Lett., vol. 16, pp. 848-851, Sept. 2016.

[15] X. Liu, S.V. Georgakopoulos, and S. Rao, "A Design of an origami Reconfigurable QHA with a Foldable Reflector," IEEE Antennas Propag. Mag., vol. 59, no. 4, pp. 78-105, Aug. 2017.

[16] G. J. Hayes, Y. Liu, J. Genzer, G. Lazzi, and M. D. Dickey, "Self-Folding origami Microstrip Antennas," IEEE Trans. Antennas Propag., vol. 62, no. 10, pp. 5416-5419, Oct. 2014.

[17] S. Yao, X. Liu, J. Gibson, S. V. Georgakopoulos, "Deployable origami Yagi loop antenna," in Proc. IEEE Antennas Propag. Soc. Int. Symp., pp. 2215-2216, Jul. 2015.

[18] J. Kimionis, M. Isakov, B. S. Koh, A. Georgiadis, and M. M. Tentzeris, "3D-printed origami packaging with inkjet-printed antennas for RF harvesting sensors," IEEE Trans. Microw. Theory Techn., vol. 63, no. 12, pp. 4521–4532, Dec. 2015.

[19] S. Alharbi, R. Shubair, and A. Kiourti, "Flexible antennas for wearable applications: recent advances and design challenges," in Proc. Europ. Conf. Antennas Propag. (EUCAP), London, UK, April 9-14, 2018.

[20] J. Zhong, A. Kiourti, T. Sebastian, Y. Bayram, and J.L. Volakis, "Conformal load-bearing spiral antenna on conductive textile threads," IEEE Antennas Wireless Propag. Lett., pp. 230–233, May 2016.

[21] Ansys High Frequency Structure Simulator. Available: https://www.ansys.com/products/electronics/ansys-hfss

[22] COMSOL Multiphysics®. Available: https://www.comsol.com/

[23] Electrisola Feindraht AG Textile Wire. Available: http://www.textile-wire.ch/

[24] A. Kiourti, C. Lee, and J.L. Volakis, "Fabrication of textile antennas and circuits with 0.1mm precision," IEEE Antennas Wireless Propag. Lett., vol. 15, pp. 151–153, 2015.

[25] Brother PE-DESIGN. Available: https://www.brother-usa.com/products/pedesign10

[26] A. Kiourti and J.L. Volakis, "High geometrical accuracy embroidery process for textile antennas with fine details," IEEE Antennas Wireless Propag. Lett., vol. 14, pp. 1474–1477, 2015.

[27] K. Karlsson, J. Carlsson, "Wideband characterization of fabrics for textile antennas," in Proc. EuCAP 2012, Prague, Czech Republic, pp. 1358 – 1361, 2012.

[28] B. Ivsic, D. Bonefacic, J. Bartolic, "Considerations of embroidered textile antennas for wearable applications", IEEE Antennas Wireless Propag. Lett., Vol.12, pp.1708 – 1711, 2013.

[29] EMSCAN RFxpert. Available: https://www.emscan.com/products/antenna-testing/